Electronic Supplementary Material (ESI) for Chemical Communications

Supporting Information

In-situ fabrication of metal-organic hybrid gel in capillary for online enrichment of trace analytes in aqueous samples

Yuling Hu, Yifen Fan, Zelin Huang, Chaoyong Song, Gongke Li**

School of Chemistry and Chemical Engineering, Sun Yat-sen University, Guangzhou, 510275， China.

1. In-situ preparation of the Fe^{3+}-BTC metal–organic hybrid gel in capillary column

Before fabrication of the metal–organic hybrid gel, the capillary was pretreated as follows. Briefly, the fused-silica capillaries (O.D. 375 μm and I.D. 320 μm), purchased from Yongnian Optic Fiber Plant (Hebei, China), were activated with 1 mol/L NaOH and then 1 mol/L HCl solution. After being rinsed with purified water and acetone respectively, it was dried at 100 ℃ in oven for 1 h.

To prepare the Fe^{3+}-BTC metal–organic hybrid gel, 100 mg of trimesic acid was first mixed adequately with the organic polymer precursor (100 μL of MAA, 400 μL of EGDMA and 15 μL of AIBN) and dissolved in 1 mL of ethanol. The obtained solution was then mixed with equal volumes of ethanolic solutions containing 300 mg $Fe(NO_3)_3$ under vigorous stirring. While the solution turned cloudy, it was immediately injected into a glass capillary at about 10 min at room temperature. Compared with the Fe^{3+}-BTC gel formed in pure ethanol, the gelation speed in presence of the organic polymer precursor was slightly reduced. Afterwards, the capillary was sealed at both ends and placed in an oven. The post-polymerization was carried out at 65℃ for 4 h to obtain a rigid metal-organic hybrid gel rod, which was washed with water, acetone, acetonitrile and methanol respectively to strip the unreacted components by a HPLC pump. The washing step proceeded until a stable baseline was monitored by UV detector.

2. Characterization of the metal–organic hybrid gel

A XL-30 scanning electron microanalyzer (Philips, Eindhoven,The Netherlands) was employed to investigate the morphological properties of the resulting metal-organic hybrid gel. The gel exhibited a rod-like shape and 3-D network skeletons with rough surface. A rigid monolith was achieved by crosslinking with the organic polymer network, whereas discontinuous gel or powered shape was obtained in ethanol without the addition of organic polymer precursor.

The infrared absorption spectrum of the metal–organic gel between 500 and 4000 cm^{-1} was obtained in an IR-prespige-21 FTIR spectrometer (Shimadzu, Japan) (Fig. S1). A broad absorption

band at 3442 cm^{-1} corresponded to the O–H stretching vibration. The stretching vibration of C=O bonds on carbonyl groups of BTC could be observed at 1734 cm^{-1}. The absorption at 1624 cm^{-1}, 1460 cm^{-1}, 1382 cm^{-1} corresponded to the C=C stretching vibration in the phenyl ring.

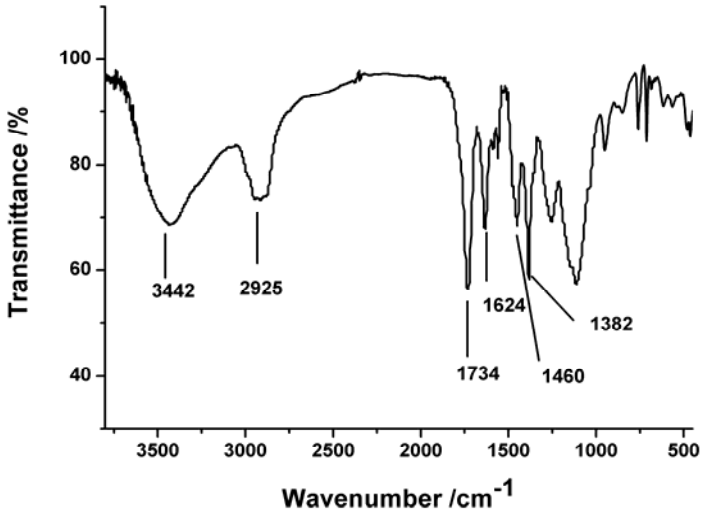

Fig. S1 The FTIR spectrum of the metal-organic hybrid gel

The chemical composition of the gel was further analyzed by X-ray photoelectron spectroscopy (XPS). As shown in Fig. S2, the iron-,oxygen- and carbon-related peaks are detected in the XPS survey spectra with the contents of C,O and Fe of 64.1 %、33.8 %、2.0 % , respectively (Fig. S2(A)). The Fe 2p spectra exhibits two intense peaks at 712.4 eV and 725.9 eV, which are positively shifted, are assigned to the specific absorption of Fe 2p1/2 and Fe 2p3/2. The observed positive shifts reveal the strong coordination interaction between Fe^{3+} and BTC (Fig. S2(B)). Analysis of the C 1s peak in Figure S2 (C) showed the presence of C-C in the phenyl ring at 284.8 eV, C–COO at 286.4 eV and the carboxylate (–COO)C 1s peak at 289.2 eV. The O1s peak at 532.2 eV is the dominant feature in the O 1s spectrum for the BTC. It is also observed an additional signal for O 1s peak appeared at 533.7 eV, which is attributed to the oxide-related species (Fe-O) (Figure S2 (D)). The results indicate that there are two different surroundings for O in the gel so that the carboxylate (–COO)O has been coordinated with Fe^{3+} in this gel material.

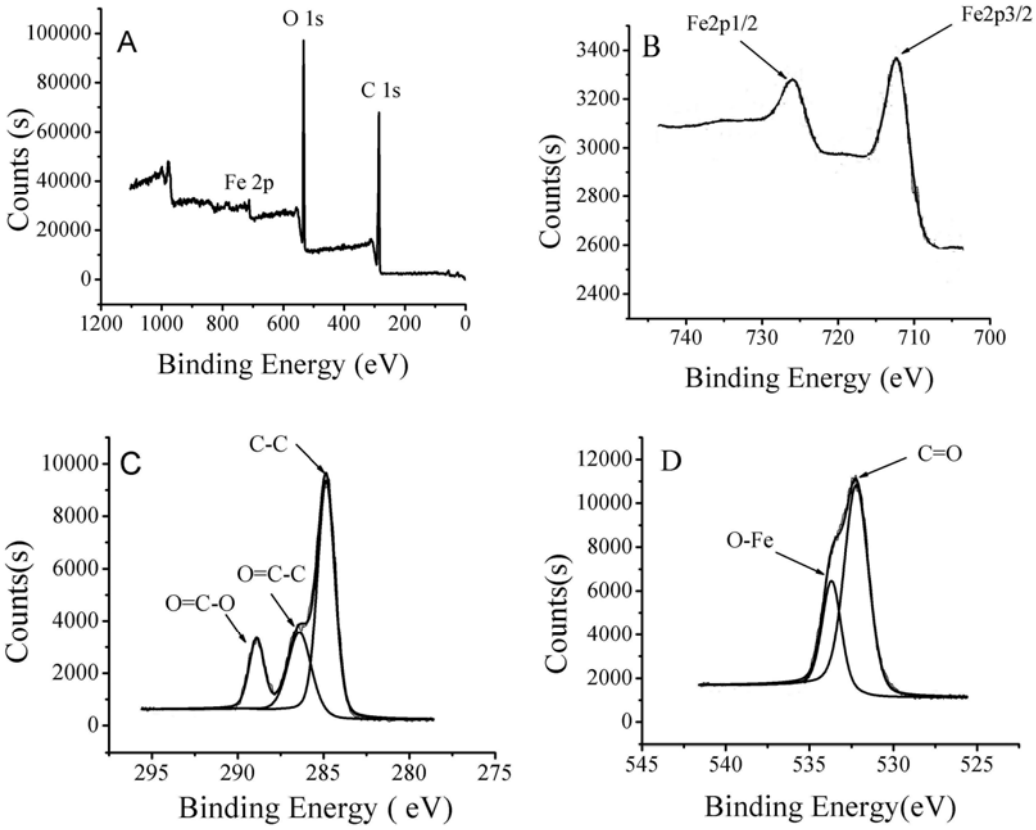

Fig. S2 X-ray photoelectron spectroscopy(XPS) spectra of the Fe^{3+}-BTC metal–organic hybrid gel (A), the Fe 2p XPS spectra (B), C1s XPS spectra (C) and O1s XPS spectra (D).

Solid-state ^{13}C NMR experiments were carried out on a Bruker Avance 400 spectrometer at frequencies of 100.61 MHz (magnetic field strength 9.4 T). The cross-polarization magic-angle spinning (CPMAS) spectra were recorded with recycle delay of 300 ms. The experiments were carried out at temperature of 292.2 K using a 4 mm CP/MAS probe. Fig. S3 shows the corresponding ^{13}C MAS spectra of the Fe^{3+}-BTC gel and the Fe^{3+}-BTC polymer hybrid gel.

It is known that the free ligand BTC has a chemical shift of 170.8 ppm for carboxylate carbon and 130-136 ppm for the aromatic carbon. However, only weak NMR signal with broad linewidth at 58.2 ppm was observed for the Fe^{3+}-BTC gel. This phenomenon might be as a result of the paramagnetic influence from Fe^{3+} when coordinated with BTC. The paramagnetic ferric ion (III) would yield a very short spin-lattice relaxation time for the ^{13}C nuclei, and make the spectrum linewidth broader. Both lead to significant decrease of the NMR signals. According to the reference (F. Gul-E-Noor, B. Jee, A. Pöppl, M. Hartmann, D. Himslb and M. Bertmer, *Phys. Chem. Chem. Phys.*, 2011, **13**, 7783–7788), the paramagnetic influence is known to strongly affect the magnetic properties of surrounding nuclei. In Fig. S3, the signal arises at 58.2 ppm might be ascribed to strong

paramagnetic shift (upfield shift of about 112 ppm) for carboxalyte carbon of BTC. The paramagnetic shift occurs due to the hyperfine interactions of the unpaired electron of Fe^{3+} with the neighboring nuclei. Although precise prediction of the paramagnetic chemical shift is difficult, the coordination interaction between Fe^{3+} and BTC can be supported by the results.

With regard to the Fe^{3+}-BTC hybrid gel, the MAA-co-EGDMA polymer was introduced to host the gel framework. Peaks were assigned by comparison with data of pure Fe^{3+}-BTC gel. The peaks at 176.8 ppm and 21.6 ppm were assigned to carbons of C=O and CH_3, respectively, in the structure of MAA-co-EGDMA polymer, because these are typical chemical shifts for those groups. The sharp peak at 45.4 ppm was assigned to the –C– carbon in the MAA-co-EGDMA polymer. Similar to Fe^{3+}-BTC gel, the typical resonances for aromatic and carboxalyte carbon in the free ligand BTC was also not observed for the hybrid gel. Instead, the broad peak at 60.6 ppm, which was assigned to the paramagnetic shift for carboxalyte carbon of BTC coordinated with Fe^{3+}, was observed. The results strongly support that the Fe^{3+}-BTC coordination polymer formed in the hybrid gel.

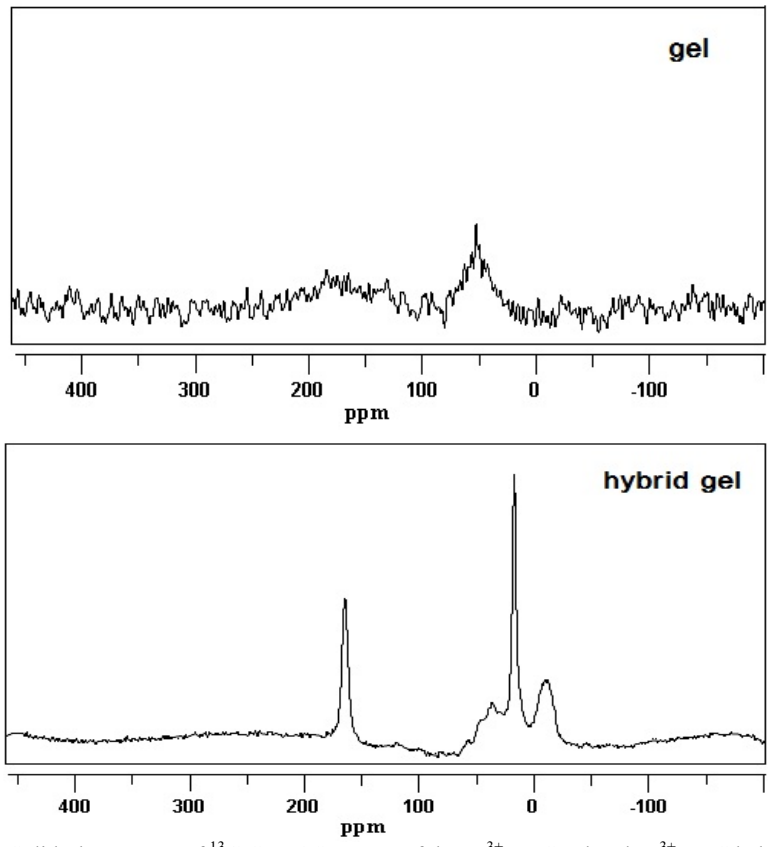

Fig. S3 Solid-phase NMR of ^{13}C CPMAS spectra of the Fe^{3+}-BTC gel and Fe^{3+}-BTC hybrid gel.

3 Construction of the in-tube solid-phase microextraction (SPME)-HPLC system for online

enrichment

The Fe^{3+}-BTC metal–organic hybrid gel capillary column was mounted on the six-way valve of the HPLC system as an online extractor. The online enrichment was realized by in-tube SPME. The schematic diagram of the in-tube SPME–HPLC system is illustrated in Fig. S4. Before extraction, valve 1 was switched to LOAD position and the carrier solution was driven by pump A to flow through the capillary for conditioning at a flow rate of 1.0 mL/min. At the same time, the sample solution was injected in the sample loop with a syringe. When extraction began, valve 1 was switched to INJECT position for a given time and then back to LOAD position thereafter. Thus, the sample solution was driven by the carrier solution to flow through the metal–organic hybrid gel capillary. After extraction, the double distilled water was kept to flow through the capillary for 1 min in order to eliminate the residual sample solution in the capillary. Finally, the extracted analytes were desorbed from the capillary to the analytical HPLC column with the mobile phase by simply switching valve 2 to INJECT position.

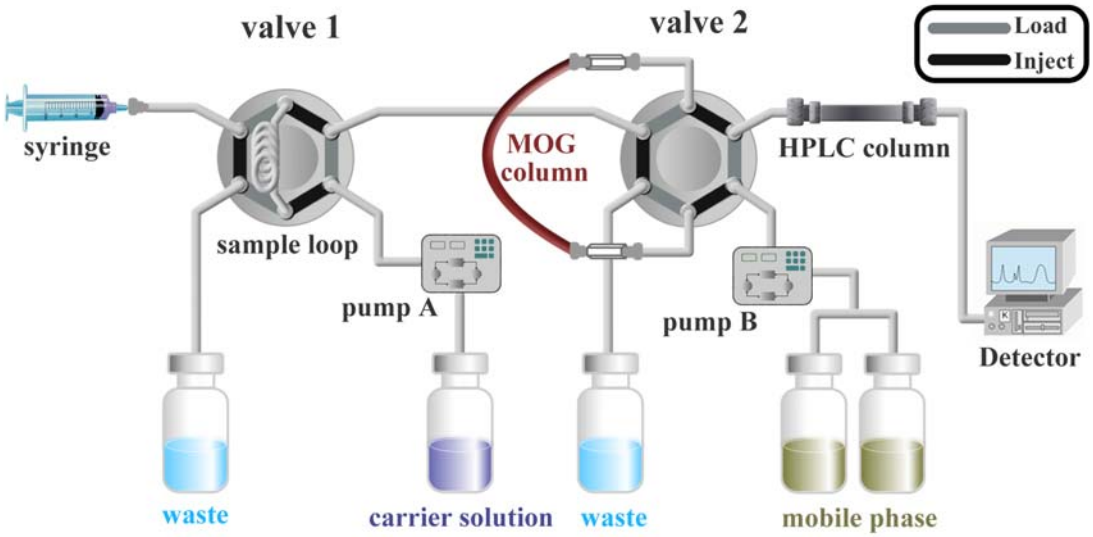

Fig. S4 The schematic diagram of the in-tube SPME–HPLC system.

4 Enrichment capability of the Fe^{3+}-BTC hybrid gel column as compared with that of the controlled polymer column without gel.

In order to illustrate the specific effect of the Fe^{3+}-BTC metal organic gel on the enrichment performance of the capillary column, we also synthesized the capillary by polymerization of the organic monomer without the presence of metal organic gel. Comparison of the extraction amounts of PAHs on the two capillary was illustrated in Fig. S5. It can be seen from Fig. S5 that the extraction amounts of the PAHs with the organometallic hybrid gel column was much higher than that with the

MAA-co-EGDMA polymer column. The excellent performance of the Fe^{3+}-BTC gel column likely resulted from the combined effects of the π-π interactions of the aromatic rings of the analytes with the framework BTC molecules, and the π-complexation of the electron-rich analytes with the Lewis acid sites in the pores of the organometallic hybrid gels. However, hydrophobic effect is dominant for the extraction of PAHs with the polymer column.

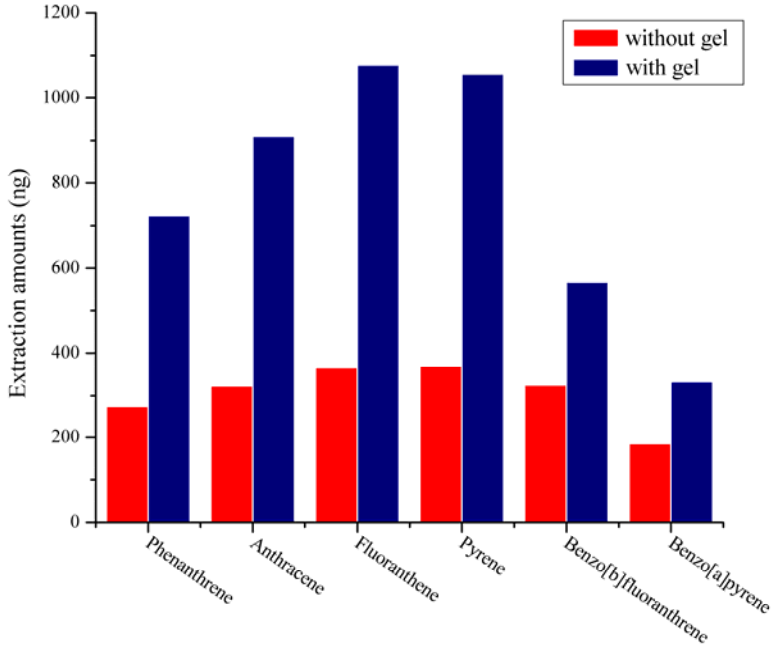

Fig. S5 Comparison of the extraction amounts of the PAHs at concentration of 10 μg/L by the Fe^{3+}-BTC hybrid gel column (with gel) and the MAA-co-EGDMA polymer column (without gel).

5 Analytical performance of the in-tube SPME-HPLC method

The developed in-tube SPME-HPLC method was applied to the determination of polycyclic aromatic hydrocarbons (PAHs) in environmental water and amphetamines drugs in urine. The analytical performance was tested regarding linearity, precision and sensitivity, which was summarized in Table S1. The sensitivity of this analytical procedure was evaluated in terms of the limit of detection (LOD) calculated using S/N=3. The analytical results of PAHs in Zhujiang River (Guangzhou, China) and the amphetamines drugs in urine from a drug abuser are shown in Table S2 and Table S3, respectively. To test the reliability of the established method, the recoveries were performed by spiking samples with standard solution at different concentrations and the results are also illustrated in Table S2 and Table S3.

Table S1 Linear regression data, detection limit and RSDs of the in-tube SPME-HPLC method

Analytes	Linear equation	r	Linear range （μg/L）	LOD （μg/ L）	RSD（%） (n=5)
Phenanthrene	Y=-745+4899X	0.9969	0.50-20.00	0.35	7.2
Anthracene	Y=-904+5784X	0.9991	0.50-20.00	0.24	7.6
Fluoranthene	Y=-4120+12677X	0.9932	0.50-20.00	0.32	6.1
Pyrene	Y=-2253+13120X	0.9920	0.50-20.00	0.24	3.9
Benzo[b]fluoranthrene	Y=2267+5153X	0.9954	0.50-20.00	0.35	6.6
Benzo[a]pyrene	Y=486+1587X	0.9990	0.50-20.00	0.40	6.2
3,4-Methylenedioxyamphetamine	Y=23+986X	0.9989	5.0-200.0	2.0	3.8
Methamphetamine	Y=-64+978X	0.9992	5.0-200.0	2.4	5.4
3,4-Methylenedioxymethamphetamine	Y=87+964X	0.9910	5.0-200.0	3.0	7.2

Table S2 Recoveries of PAHs in river water samples.

Analytes	Detected	Spiked with 1.0 μg/L		Spiked with 5.0 μg/L	
		Recovery (%)	RSD (%) (n=3)	Recovery (%)	RSD (%) (n=3)
Phenanthrene	N.D	93.6	5.9	91.0	6.6
Anthracene	N.D	106.1	2.9	91.5	6.2
Fluoranthene	N.D	108.5	4.6	104.5	2.3
Pyrene	N.D	87.3	4.8	102.0	1.4
Benzo[b]fluoranthrene	N.D	100.8	8.3	89.2	8.0

Table S3 Recoveries of the amphetamines drugs in urine

Analytes	Detected	Spiked (μg/L)	Recovery (%)	RSD (%) (n=3)
3,4-Methylenedioxyamphetamine	N.D	100.0	81.1	2.1
Methamphetamine	N.D	100.0	74.3	6.2
3,4-Methylenedioxymethamphetamine	94.4±4.6	100.0	108.2	3.3